ELSEVIER

Physica D 163 (2002) 94–105

PHYSICA D

www.elsevier.com/locate/physd

The bifurcation diagrams for the Ginzburg–Landau system of superconductivity

Amandine Aftalion [a,*], Qiang Du [b]

[a] *CNRS et Laboratoire d'Analyse Numérique, B.C. 187, Université Pierre et Marie Curie, 4 Place Jussieu, 75252 Paris Cedex 05, France*
[b] *Department of Mathematics, Hong Kong University of Science and Technology, Clear Water Bay, Kowloon, Hong Kong, PR China*

Received 20 February 2001; received in revised form 26 September 2001; accepted 28 November 2001
Communicated by R. Temam

Abstract

In this paper, we provide the different types of bifurcation diagrams for a superconducting cylinder placed in a magnetic field along the direction of the axis of the cylinder. The computation is based on the numerical solutions of the Ginzburg–Landau model by the finite element method. The response of the material depends on the values of the exterior field, the Ginzburg–Landau parameter and the size of the domain. The solution branches in the different regions of the bifurcation diagrams are analyzed and open mathematical problems are mentioned. © 2002 Elsevier Science B.V. All rights reserved.

Keywords: Ginzburg–Landau model; Superconductivity; Finite element method

1. Introduction

In this paper, we want to give a detailed description of the bifurcation diagrams of an infinite superconducting cylinder of cross-section Ω, submitted to an exterior magnetic field h_0. The response of the material varies greatly according to the value of h_0, the size of the cross-section and the Ginzburg–Landau parameter κ that characterizes the material: superconductivity appears in the volume of the sample for low fields and small samples, under the form of vortices for higher fields, bigger samples and larger values of κ, and is destroyed for high fields. The type of response of a superconducting material has been studied numerically and theoretically by various authors in various asymptotic regimes [2,4,7,8,11–14,18,19,23,28–31,33–37]. Here, we want to give a complete numerical picture of the bifurcation diagrams for all values of the parameters. This type of computation has already been done in dimension 1 by one of the authors using auto [3]. Here, the computation is made in a two-dimensional domain using numerical solutions of the well-known Ginzburg–Landau model [38] based on a code first developed in [18]. We examine the behavior of the energy, the magnitude of the order parameter and the magnetization versus the magnetic field for various solution branches. We also provide some analysis on the detailed findings such as the stability of solutions.

The paper is organized as follows: the Ginzburg–Landau model is briefly stated in Section 2 and the main features of the numerical codes used in the computation are described in Section 3. The complete phase diagrams are given in Section 4 along with detailed analysis. A conclusion is given in Section 5.

* Corresponding author. Tel.: +33-1-4427-8519; fax: +33-1-4427-7200.
E-mail address: aftalion@ann.jussieu.fr (A. Aftalion).

0167-2789/02/$ – see front matter
PII: S0167-2789(01)00385-2

2. The Ginzburg–Landau model

Let Ω denote a two-dimensional bounded domain which represents the cross-section of a three-dimensional cylinder occupied by the superconducting sample. Assume that the cylinder is homogeneous along its axis and a constant applied field H_0 is placed along the axis direction as well. Then, the Gibbs free energy $\mathcal{G}$ may be written in the following form [38]:

$$\mathcal{G}(\psi, A) = \int_\Omega \left(f_n + \alpha|\psi|^2 + \frac{\beta}{2}|\psi|^4 \right) \mathrm{d}\Omega + \int_\Omega \left[\frac{1}{2m_\mathrm{s}} \left| \left(\mathrm{i}\hbar\nabla + \frac{e_\mathrm{s}A}{c} \right) \psi \right|^2 + \frac{|\mathrm{curl}\, A|^2}{8\pi} - \frac{\mathrm{curl}\, A \cdot H_0}{4\pi} \right] \mathrm{d}\Omega.$$

Here, ψ is the (complex-valued) order parameter, A the magnetic potential, curl A is the magnetic field, α and β are constants (with respect to the space variable x) whose values depend on the temperature, c the speed of light, e_s and m_s are the charge and mass, respectively, of the superconducting charge-carriers, and $2\pi\hbar$ is the Planck's constant.

After proper nondimensionalization, we can reformulate the free energy functional as:

$$\mathcal{G}(\psi, A) = \int_\Omega |(\nabla - \mathrm{i}A)\psi|^2 + \frac{\kappa^2}{2}(1 - |\psi|^2)^2 + |\mathrm{curl}\, A - h_0|^2 \, \mathrm{d}\Omega,$$

where κ is the Ginzburg–Landau parameter representing the ratio of the penetration depth and the coherence length, h_0 the applied magnetic field and d the characteristic size of the domain Ω, i.e. $\Omega = dD$, where D is a fixed domain.

The system that we are going to study is the following Ginzburg–Landau equations derived as the Euler–Lagrange equations for the minimizers of the functional $\mathcal{G}$ [22]:

$$\begin{aligned} &-(\nabla - \mathrm{i}A)^2\psi = \kappa^2\psi(1 - |\psi|^2) \ \text{ in } \ \Omega, \\ &-\mathrm{curl}\,\mathrm{curl}\, A = |\psi|^2 A + \frac{\mathrm{i}}{2}(\psi^*\nabla\psi - \psi\nabla\psi^*) \ \text{ in } \ \Omega, \end{aligned} \tag{1}$$

which are supplemented by the boundary conditions

$$(\nabla\psi - \mathrm{i}A\psi) \cdot n = 0 \ \text{ on } \ \partial\Omega,$$

$$\mathrm{curl}\, A = h_0 \ \text{ on } \ \partial\Omega,$$

and gauge constraints

$$\mathrm{div}\, A = 0 \ \text{ in } \ \Omega, \qquad A \cdot n = 0 \ \text{ on } \ \partial\Omega.$$

Here, $\partial\Omega$ is the boundary of Ω and n its unit outer normal. With the above nondimensionalization, $|\psi|$ takes values between 0 and 1; the normal state corresponds to $|\psi| = 0$ while the Meissner state corresponds to $|\psi| = 1$.

This Ginzburg–Landau model has a special family of solutions called the *normal solutions*: $\psi = 0$ and curl $A = h_0$, which correspond to the situation where superconductivity is destroyed. According to the values of the different parameters κ, d and h_0, the system may have other solutions: *superconducting solutions*, for which ψ is never 0 and *vortex solutions* for which ψ has isolated zeroes (see Figs. 1 and 2). For a complete introduction to the topic, one may refer to [38].

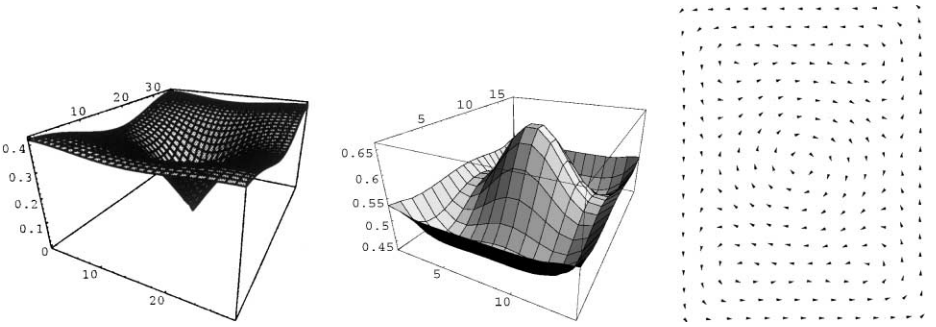

Fig. 1. A single vortex solution of (1).

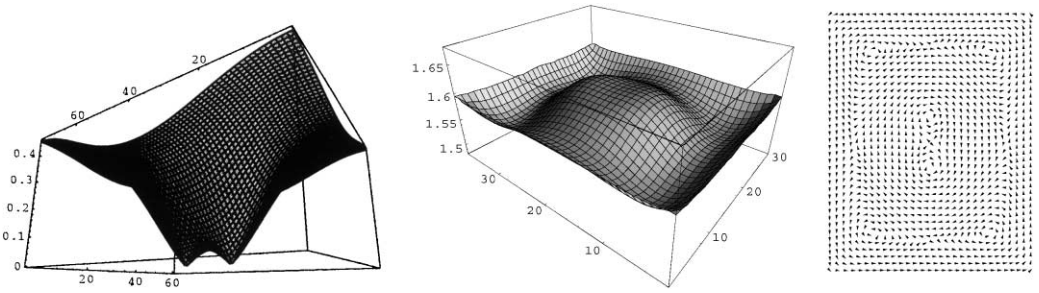

Fig. 2. A solution of (1) with two vortices.

3. Numerical codes

The numerical code that we are using is based on the finite element approximations of the Ginzburg–Landau model, first proposed in [18] and later used in many settings, see [19,26,39] for instance. The codes have many different variants that can be used to simulate the solutions of the Ginzburg–Landau model in the high κ setting [11,17], thin films with variable thickness [10], samples with normal inclusions [19] as well as layered materials. Here, we choose the standard version that solves the Ginzburg–Landau equations on a rectangular domain Ω and d will denote the characteristic size of the rectangle. We note that other numerical methods, such as the gauge invariant difference methods [16], i.e. the so-called bond-and-link variable methods or the method of eigenfunctions, have also been used to compute the phase diagrams for the Ginzburg–Landau equations [6,15].

In our implementation of the finite element approximation, we use a uniform triangular grid with piecewise quadratic polynomials for both ψ and A. It is shown that (see [18] for instance), if (ψ_δ, A_δ) is the finite element solution on a given mesh with mesh size δ, the convergence of the approximation is assured, and asymptotically, we have

$$\|\psi - \psi_\delta\|_2 + \|A - A_\delta\|_2 = \mathrm{O}(\delta^3),$$

where $\|\cdot\|_2$ denotes the standard mean square L^2 norm. For each set of calculation, we refine the mesh size until numerical convergence is evident.

In Figs. 1 and 2, we present a few typical plots for the numerical solutions of Eq. (1). For each solution, the plots include a surface plot of the magnitude of the order parameter, a surface plot of the magnetic field given by curl A and a vector plot of the superconducting current. In Fig. 1, we have a solution with a single vortex at the center of the domain which corresponds to the parameter values $\kappa = 0.23$, $d = 16.8$ and $h_0 = 0.563$.

In Fig. 2, we present the plots for a solution with two vortices corresponding to $\kappa = 0.8$, $d = 4$ and $h_0 = 1.2$.

For fixed κ, d and h_0, we are interested in finding the number of solutions of (1) and their stability. A continuation in the parameter spaces is used for getting solutions with different parameter values. With κ, d given but h_0 allowed to vary, for a computed solution branch, we plot $\|\psi\|_\infty$, the maximum magnitude of the order parameter ψ in the domain, the free energy $\mathcal{G}$ and the magnetization versus the applied field h_0. These phase diagrams or bifurcation diagrams will give us information on the solutions (number and stability) for each h_0. They were drawn by Ginzburg [21] in some limiting cases of the parameters. Here we want to give a more complete description of these diagrams for all values of the parameters.

The results of our numerical computations allow us to separate the κ–d plane into different regions depending on the shape of the bifurcation diagram. A solution branch may exist in one region but may cease to exist in another one, it may also develop hysteresis in some regions.

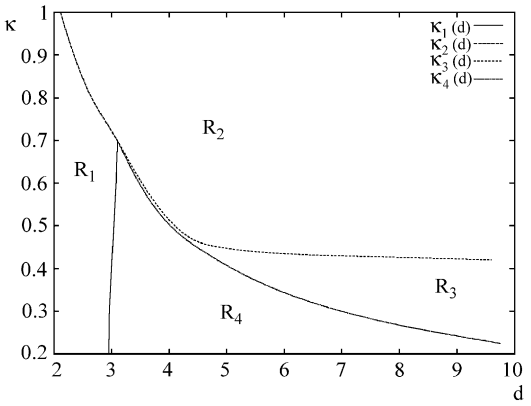

Fig. 3. The curves $\kappa_1(d)$, $\kappa_2(d)$, $\kappa_3(d)$ and $\kappa_4(d)$.

4. The bifurcation diagrams

It is well known that for large fields ($h > h_*$), the only solution is the normal solution [23]. For smaller fields ($h < h_*$), the normal solution always exists but there are other solutions which display four different types of behaviors. These behaviors depend on the values of κ and d. In Fig. 3, we have plotted four curve segments $\{\kappa_i(d)\}_1^4$ separating the κ–d plane into four regions $\{R_i\}_1^4$.

The four curve segments in Fig. 3 are the results of the computation described in the earlier section. All four curves meet close to $\kappa = 1/\sqrt{2}$, $\kappa_2(d)$ is of the form $2.112/d$, $\kappa_3(d)$ is tending to 0.4 at infinity. The four regions correspond to the four types of behaviors for the bifurcation diagrams. For convenience, for each $i = 1, 2, 3, 4$, we use $d = d_i(\kappa)$ to denote the inverse function of the function $\kappa = \kappa_i(d)$ wherever the inverse is well-defined. What distinguishes the different regions are features like the existence (or the lack of existence) of vortex solutions, the global and local stability of solutions and the hysteresis phenomena.

We now provide detailed descriptions of the solution behavior for each region in Fig. 3.

Region 1: $d < d_1(\kappa)$ *and* $d < d_2(\kappa)$. This corresponds to the situation where the cross-section of the superconducting sample is small enough. The bifurcation diagram is illustrated in Fig. 4. The corresponding plot of the energy is given in Fig. 5 and the magnetization curve in Fig. 6.

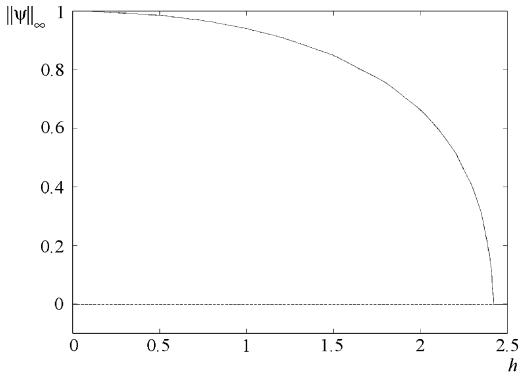

Fig. 4. The bifurcation curve for $d = 2.0$ and $\kappa = 0.3$.

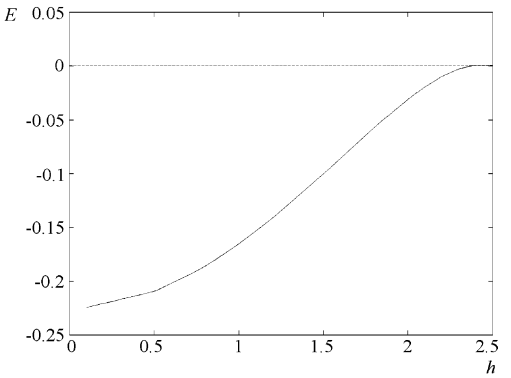

Fig. 5. The energy for $d = 2.0$ and $\kappa = 0.3$.

Throughout this region, there is a unique nonnormal solution for $h < h_*$. This solution is a superconducting solution which is the global minimizer of the free energy $\mathcal{G}$. The curve $\|\psi\|_\infty$ against h is monotonically

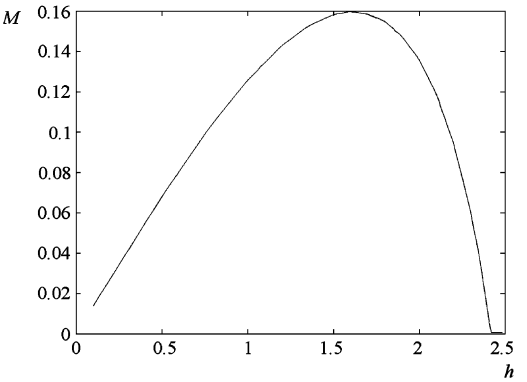

Fig. 6. The magnetization for $d = 2.0$ and $\kappa = 0.3$.

decreasing. When increasing the field, the magnitude of the superconducting solution decreases until it turns normal at $h_0 = h_*$. Conversely, when decreasing the field, the normal solution turns superconducting also for $h_0 = h_*$. The transition to the normal solution is of second-order, i.e. the energy of the superconducting solution tends to the energy of the normal solution at the transition and there is no hysteresis phenomenon. This can also be seen on the magnetization curve of Fig. 6.

There is no vortex solution for the parameters (d, κ) in this region. This reflects the fact that d is too small to allow enough room for a vortex to exist since a vortex core is of typical size C/κ.

In [2], it is proved that for $d < \min\{d_0, d_1/\kappa\}$, a solution of the Ginzburg–Landau equations has no vortex, and for such a solution, ψ is almost constant in the domain and is unique up to multiplication by a constant of modulus 1. Also it is proved that the bifurcation curve for $\|\psi\|_\infty$ is decreasing and that h_* is asymptotically C/d when d tends to 0. More precisely, for a disk, when d tends to 0, the limiting curve is $\|\psi\|_\infty^2 = 1 - d^2 h_0^2/2\kappa^2$.

Region 2: $\kappa > \kappa_2(d)$ *and* $\kappa > \kappa_3(d)$. In contrast with Region 1, this region corresponds to the situation where the typical size of vortices (C/κ) is small enough compared to the size of the domain. This region displays the typical type II behavior of superconductors. The bifurcation diagram is illustrated in Fig. 7, the energy in Fig. 8 and the magnetization curve is given in Fig. 9.

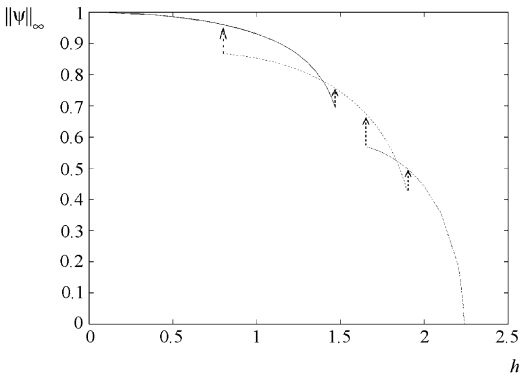

Fig. 7. The bifurcation curve for $d = 3.2$ and $\kappa = 1$.

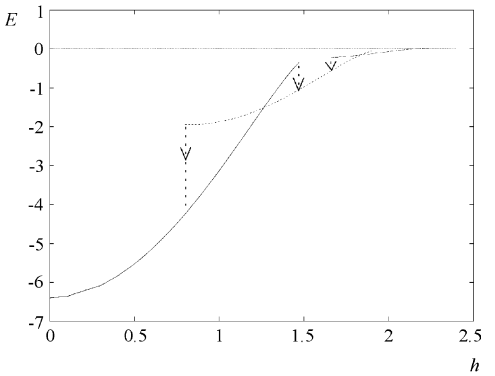

Fig. 8. The energy for $d = 3.2$ and $\kappa = 1$.

It has been well understood both physically and in more recent years mathematically that, for sufficiently large κ, there are vortex solutions which are the global minimizers of the free energy for a certain range of fields. The number of vortices depends on the strength of the applied field. The maximum number of vortices increases with d and κ, a type II behavior.

For very small fields, the global minimizer is the superconducting solution (solid line). As the field is increased, the superconducting solution loses its global stability ($h = h_{c_1}$ and for even larger fields loses its local stability, $h = h_0^*$). Then the global minimizer starts to nucleate vortices. In Figs. 7–9, the solution branch corresponding to a one vortex solution is illustrated by a dotted line and to a two vortex solution by a dashed line.

Let n be a nonnegative integer (the flux quanta). Hysteresis phenomena occur in our experiments when

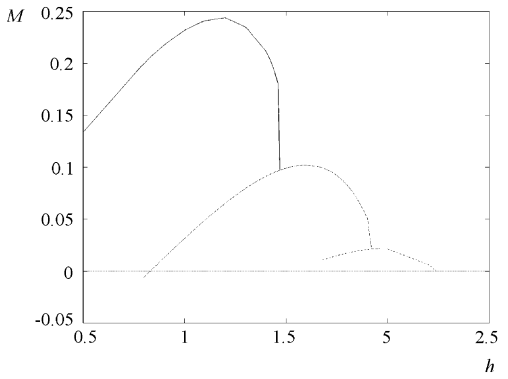

Fig. 9. The magnetization for $d = 3.2$ and $\kappa = 1$.

going from a solution with n vortices to a solution with $n+1$ vortices: when increasing the field, the solution with n vortices remains locally stable, though it is no longer a global minimizer until h_n^* where it jumps to a solution with $n+1$ vortices. Similarly when decreasing the field, the solution with $n+1$ vortices remains locally stable down to $h_*^{n+1} < h_n^*$. Such a hysteresis pattern is typical for parameters in this region. The fields h_n^* and h_*^{n+1} correspond to the critical field where the vortex solution loses its local stability and their values can be identified from Figs. 7 and 8 (transition from superconducting solution to 1 vortex solution and from one vortex to two vortices).

Nevertheless, the transition from normal to the last vortex solution is of second-order since the vortex solution is stable, as can be seen from the energy and magnetization curves. This transition occurs at a field that is usually called h_{c_3} in the literature.

There have been many numerical works on these vortex solutions: see for instance [14,36,37]. In [37], the phenomena of bifurcation from normal state to giant vortex and from giant vortex to single vortices is largely studied and this refine our analysis or Region 2. Recently, a rigorous analysis of vortices, their number and the critical thermodynamic fields in the high kappa limit has been done by Sandier and Serfaty [33–35], in particular they obtain in the high kappa limit that h_{c_1} (the field for which the energy of the superconducting solution is equal to the energy of the one vortex solution) is of order $C\log\kappa$ and the field h_n^* is asymptotic to $h_{c_1} + n\log\log\kappa$. Another study has been made by Akkermans and Mallick [4] for κ close to $1/\sqrt{2}$; they are able to compute the energy as a function of the applied field and they find that the profile is parabolic as illustrated in Fig. 8.

The onset of superconductivity in decreasing fields (instability of normal solutions and computation of the fields of nucleation) has been analyzed by Bernoff and Sternberg [8] and Del Pino et al. [13]. Other works concerning the linearized problem include [24,28,29] and also [25,30] in dimension 3. Their works provide, as d and κ tends to ∞, an asymptotic development of h_{c_3}, the field at which the normal solution bifurcates to a vortex solution. This is what is called surface superconductivity. Linearizing the Ginzburg–Landau equation has been done near the normal solution. In the high kappa limit, their computation yields

$$h_{c_3} \sim \frac{\kappa^2}{\lambda_1} + C\kappa\kappa_{\max} + \mathrm{o}(\kappa), \tag{2}$$

where $\kappa_{\max}$ is the maximal curvature of the domain and λ_1 is the first eigenvalue of the linearized problem and is approximately equal to 0.59. In the high d limit, it yields

$$h_{c_3} \sim \frac{\kappa^2}{\lambda_1} + \frac{C\kappa\kappa_{\max}}{d^2} + \mathrm{o}\left(\frac{1}{d^2}\right). \tag{3}$$

This expansion is consistent with the work of Saint-James and De Gennes [32] who got the first term of this expansion in the case of an infinite plane in one dimension. This work in one dimension was made rigorous by [9]. In two dimensions, one has to take into account the curvature of the cross-section. In the case of the disk, the equivalent of expansions (2) and (3) have been carried out by [7] in the limit κd is large.

Pan [31] has rigorously analyzed the state of the material when the magnetic field is further decreased from the nucleation. He proves that the wave function ψ is nonzero in a uniform neighborhood of the boundary.

The hysteresis phenomenon has been rigorously analyzed in [27] for the superconducting solution $(n=0)$.

Some interesting questions to be addressed here are: what are the critical fields for the vortex solutions losing their local stability (h_n^* and h_*^n)? Can we find them in some asymptotic limit such as d large or κ large or κd large? Can we prove the existence of these hysteresis phenomena for the general case?

Curve $\kappa_2(d)$. For fixed κ above 0.7, when d is increased from 0, the point (d,κ) is first in Region 1. Then it reaches the critical value $d_2(\kappa)$. For $d = d_2(\kappa)$, the bifurcation diagram $\|\psi\|_\infty$ versus h is decreasing and the superconducting solution bifurcates from the normal solution at $h = h_*$. For d a little larger than $d_2(\kappa)$, there is a vortex solution bifurcating from the normal solution close to h_*. Hence for $d = d_2(\kappa)$, at $h = h_*$, the linearized problem near the normal state has two eigenfunctions: one without vortices and one

with a vortex. This is how uniqueness of solution is lost when increasing d, though the assertion need to be proved mathematically.

Let D be the fixed domain such that $\Omega = dD$. Then a bifurcated solution near the normal state $(0, h_0 a_0)$ (where a_0 is such that $\operatorname{curl} a_0 = 1$ in D and $a_0 n = 0$ on $\partial\Omega$) is of the form $(\varepsilon\phi, h_0 a_0 + \varepsilon B)$. Let $\omega = h_0 d$. The second variation of $\mathcal{G}$ near the normal state is

$$\frac{\partial \mathcal{G}^2}{\partial \varepsilon^2}(\varepsilon\phi, h_0 a_0 + \varepsilon B) = \frac{1}{d^2}\int_D |(\mathrm{i}\nabla + \omega^2 a_0)\phi|^2 - \kappa^2 d^2 |\phi|^2 + |\operatorname{curl} B|^2.$$

Let

$$\lambda(\omega) = \inf\left(\int_D |(\mathrm{i}\nabla + \omega^2 a_0)\phi|^2,\ \|\phi\|_{L^2} = 1,\ \phi \in H^1(D, \mathbb{C})\right).$$

Hence, if $\lambda(\omega) > \kappa^2 d^2$, the normal solution is stable, if $\lambda(\omega) < \kappa^2 d^2$, the normal solution is unstable and if $\lambda(\omega) = \kappa^2 d^2$, degenerate stability occurs. For the eigenvalue $\lambda(\omega) = \kappa^2 d^2$, bifurcation of nonnormal solutions occurs. Thus, one has to study

$$\begin{aligned} &(\nabla - \mathrm{i}\omega^2 a_0)^2 \phi = \lambda(\omega)\phi \ \text{ in } \ D, \\ &\frac{\partial \phi}{\partial n} = 0 \ \text{ on } \ \partial D, \end{aligned} \tag{4}$$

with $\lambda(\omega) = \kappa^2 d^2$. For most values of κ and d, the field h such that the first eigenvalue $\lambda(\omega)$ is equal to $\kappa^2 d^2$ yields a single eigenfunction. In Region 1, the eigenfunction has no vortex while in Region 2, the eigenfunction has a vortex. Thus, the curve $\kappa_2(d)$ corresponds to those values of κ and d for which the eigenvalue has two different eigenfunctions, one without vortices and one with a vortex, i.e. on $\kappa_2(d)$, the vortex state starts to exist.

This situation has been studied in the case of a ball in [7]. See also [5] for more recent developments. In this case, the solutions of (4) with n vortices are of the form $\xi_n(r)\exp(\mathrm{i}n\theta)$ and have eigenvalue $\lambda(\omega, n)$. In particular, in [7] they draw the function $\lambda(\omega, n)$ versus ω. The curves $\lambda(\omega, 0)$ and $\lambda(\omega, 1)$ intersect exactly once for $\omega = \omega_0$ and $\lambda = \lambda_0$. Because of the bifurcation condition $\lambda(\omega) = \kappa^2 d^2$, it implies that $\kappa^2 d^2 = \lambda_0$, hence the curve $\kappa_2(d)$ is of the form $\kappa d =$ constant. It would be interesting to give a rigorous proof that the curves $\lambda(\omega, 0)$ and $\lambda(\omega, 1)$ intersect only once for the case of the disk and for the case of a more general domain. In Region 1, that is below $\kappa_2(d)$, the first eigenfunction is simple and leads to a solution without vortex. In Region 2, that is above $\kappa_2(d)$, the first eigenfunction is simple and leads to a solution with one vortex, but we expect that there is also an eigenfunction with no vortex for a lower field h.

Similarly, the curves $\lambda(\omega, n)$ and $\lambda(\omega, n+1)$ also intersect only once on the numerics of [7] which means in our setting that there are curves $\kappa d = C_n$ at which the eigenvalue has two eigenfunctions with n and $n+1$ vortices. Above $\kappa d = C_n$, a solution with $n+1$ vortices starts to bifurcate from the normal state and below it, a solution with n vortices starts to bifurcate from the normal state, so that the curve $\kappa d = C_n$ are the critical curves for the existence of $n+1$ vortices.

In the general case that we are studying, it is totally open to prove that there is a unique value of ω such that $\lambda(\omega)$ has two eigenvalues, one with a vortex and one without. This would yield to $\kappa_2(d) = C/d$, which is what we have found numerically. Moreover, we observe that the field of bifurcation h_* satisfies $h_* d = \omega$ hence is constant along $\kappa_2(d)$.

Taking this analysis of bifurcation a little further allows us to define

$$\mathcal{H}(\kappa, d) = \{h, \text{s.t. } \lambda(\sqrt{hd}) = \kappa^2 d^2\}.$$

In Region 1, we expect that $\mathcal{H}$ has a single element while in Region 2, we expect this set to have several elements corresponding to the various branches of solutions with several vortices bifurcating from the normal state. But this analysis is open even in the case of the disk.

Region 3: $\kappa_4(d) < \kappa < \kappa_3(d)$. For parameters in this region, i.e. large domains and intermediate κ (in a relative sense), a typical phase diagram is illustrated in Fig. 10 with the energy in Fig. 11 and the magnetization in Fig. 12. Three solution branches are shown which represent the normal solution, the superconducting solution (solid line) and a solution with a single vortex (dashed line). A profile for one of the vortex solutions is given in Fig. 1.

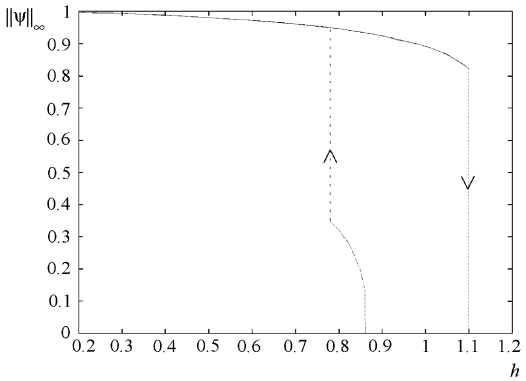

Fig. 10. The bifurcation curve for $d = 6.274$ and $\kappa = 0.35$.

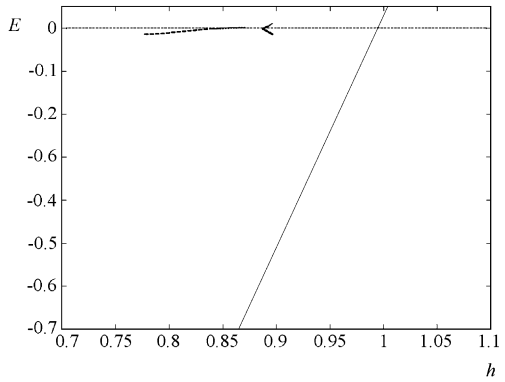

Fig. 11. The energy for $d = 6.274$ and $\kappa = 0.35$.

The superconducting solution displays a hysteresis behavior as before, but when increasing the field, it turns normal instead of going on the vortex branch as in Region 2. More precisely, as the field is increased, the superconducting solution loses its global stability, then its local stability and its drops to the normal branch when the super-heating field is reached. Conversely, when decreasing the field from the normal state, the solution gets on the vortex branch, though it is only a local minimizer. So the transition when going down the field is of second-order as can be seen on the magnetization curve (Fig. 12), but when going up, there is a hysteresis. When decreasing the field further, the solution jumps to the superconducting branch. The vortex solution is never a global minimizer. In fact, our numerical experiments indicate that there are only locally stable vortex solutions. Such behavior as in Fig. 12 had already been observed in [36].

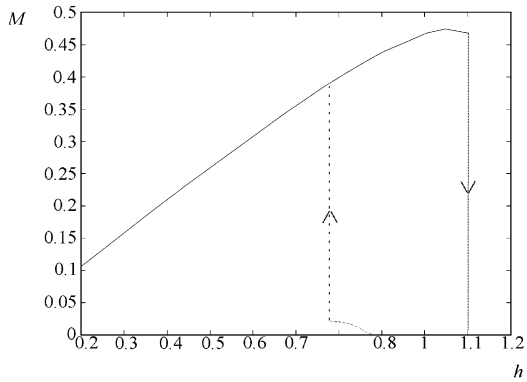

Fig. 12. The magnetization for $d = 6.274$ and $\kappa = 0.35$.

We note that, for values of the Ginzburg–Landau parameter κ in this region, the vortex state has not been frequently studied in the literature, except for superconducting sample with extreme geometrical conditions such as thin films, disks and rings. In the latter cases, the material displays typical type II behavior for all ranges of κ as the Ginzburg–Landau model can be simplified to allow an almost uniform penetration of the magnetic field [10]. However, the current study is done for three-dimensional infinite cylinders and the simplified models are not directly applicable. In fact, from the plot of the magnetic field given in Fig. 1, we see that there is considerable variation in the field strength over the cross-section.

Curve $\kappa_3(d)$. Let us call H_c, the thermodynamic critical field introduced by Ginzburg [21]: the energy of the superconducting solution is equal to the energy of the normal solution at this field (in our nondimensionalization, it means that the energy of the superconducting solution is 0). The curve $\kappa_3(d)$ corresponds to the situation where there is a small amplitude vortex solution bifurcating from the normal solution exactly at H_c. One could hope to determine this curve mathematically.

We notice that as d tends to infinity, $\kappa_3(d)$ tends to a finite limit close to 0.4 which is less than $1/\sqrt{2}$. Using (3), one can get that in the high d limit, κ is close to $\lambda_1 H_c$, where λ_1 is the first eigenvalue of the linearized problem (4) in an infinite domain and is close to 0.59. In Ginzburg's [21] computations (see also [38]), H_c is exactly $1/\sqrt{2}$ in the limit $d = \infty$. This gives $\lambda_1/\sqrt{2}$

as a limit for $\kappa_3(d)$ at infinity, which is close to 0.42. A rigorous mathematical justification of this asymptotic behavior remains to be provided.

Let us recall that the critical value of κ equal to $1/\sqrt{2}$ that separates type I and type II superconductors was discovered by Ginzburg studying the bifurcation of the *superconducting* solution from the normal state for an infinite domain. Then Saint-James and De Gennes discovered surface superconductivity, i.e. superconductivity is nucleated first in the surface and thus appears for higher fields than that was calculated by Ginzburg. Here, we see that for κ less than $\kappa_3(d)$, the vortex solution is no longer stable but is locally stable near the bifurcation.

Region 4: $\kappa < \kappa_4(d)$ *and* $d > d_1(\kappa)$. For parameters in this region, i.e. κ small but domains large enough, the typical bifurcation diagram is illustrated in Fig. 13 with the energy in Fig. 14 and the magnetization in Fig. 15.

There are superconducting solutions displaying a hysteresis phenomenon and no locally stable vortices. The superconducting solution is not always the global minimizer, but when increasing the field, the sample remains superconducting until reaching a super-heating field h^*, where the solution becomes normal with a discontinuous transition. Similarly, when decreasing the field, the sample stays normal until the field h_* which is less than h^*, where it turns superconducting by a discontinuous transition. Mathematically, we believe that there is a range of fields, between h_* and h^* where there are multiple

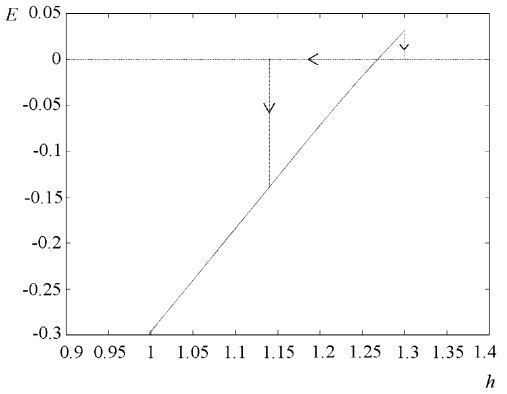

Fig. 14. The energy for $d = 4$ and $\kappa = 0.3$.

superconducting solutions. This is in analogy with what happens for the one-dimensional case. For more rigorous analysis of the one-dimensional models, we refer to [3].

Next, we also note that there is no locally stable vortex solution in the region. It is well-known that asymptotically for small κ, the vortex solution is not energetically favorable, and the material belongs to the typical type I regime [20,38] where the phase transition is characterized by the superconducting/normal interface rather than the vortex state. When varying the field, the superconducting or normal solutions will not turn into a one vortex solution. However, if we do continuation from a vortex solution for a bigger value of κ (in Region 3), and decrease κ, we can still find existence of solutions with vortices when we

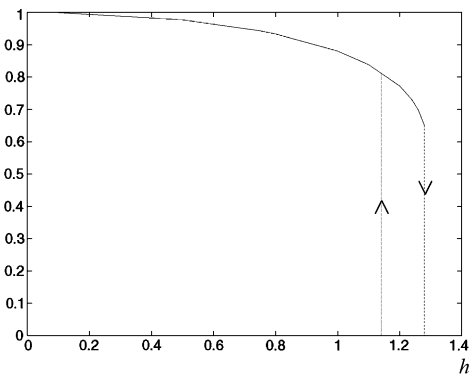

Fig. 13. The bifurcation curve for $d = 4$ and $\kappa = 0.3$.

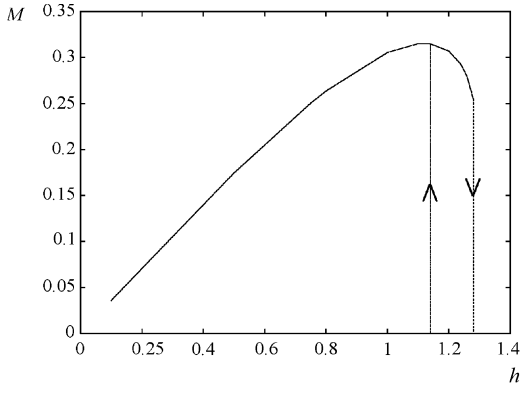

Fig. 15. The magnetization for $d = 4$ and $\kappa = 0.3$.

reduce κ to values in Region 4 despite the instability of vortex solutions. For even smaller κ, continuations in κ or in other parameters from the vortex solutions fails to produce any new vortex solutions. We believe that when decreasing κ, the vortex solution first loses its stability near the normal solution (on the curve $\kappa_4(d)$), but it remains locally stable for $\|\psi\|_\infty$ a little higher in the branch. For very small κ (especially less than C/d), we believe that there is no vortex solution at all. This has been proved in [7] in the case of a disk. It is an open problem to prove that for fixed d and for κ small enough, vortex solutions do not exist.

Curve $\kappa_1(d)$. If κ is fixed below 0.7 and d is increased, then the curve $d_1(\kappa)$ is crossed. It remains establish the mathematical existence of this curve. In the particular case where κ is very small, the order parameter ψ is almost constant, there are no vortices in the domain so that system (1) simplifies to

$$\Delta A = |\psi|^2 A, \ \text{ in } \ \Omega \qquad \operatorname{curl} A = 1 \ \text{ on } \ \partial\Omega,$$

where $|\psi|$ is a constant that depends on h_0. The boundary condition for ψ yields $\int |\psi|(|\psi|^2 + h_0^2 A^2 - 1) = 0$, which is the equation of the bifurcation curve. One has to find the critical d for which the curve $|\psi|(h_0)$ changes direction of bifurcation near $|\psi| = 0$, so that the bifurcation goes from stable for small d to unstable for larger d. Another way to study this curve is to make the bifurcation analysis near the normal state, described in the analysis of $\kappa_2(d)$, which yields to (4). Then one would need to take this development to higher order to get the sign of energy of the bifurcated branch. This sign changes on $\kappa_1(d)$. The fact that the bifurcation from the normal state is unstable for large d has not been studied.

Curve $\kappa_4(d)$. Another open problem is to determine the behavior of $\kappa_4(d)$ as d tends to infinity. We expect it to be of the order C/d for some constant C. We believe that the analysis that we have explained for the curve $\kappa_2(d)$ is the same here, i.e. on $\kappa_4(d)$ as well the eigenvalue has two eigenfunctions. The same analysis of the linearized problem needs to be performed. The difference with $\kappa_2(d)$ is that the eigenfunction with no vortex is stable on $\kappa_2(d)$ and unstable on $\kappa_4(d)$.

The point of intersection. Note that all curves $\kappa_i(d)$ intersect at the same point. Indeed the point of intersection of $\kappa_2(d)$ and $\kappa_4(d)$ has an eigenvalue with two eigenfunctions, one of which (the one without vortices) changes stability. Hence this point also belongs to $\kappa_1(d)$ since on $\kappa_1(d)$ the stability of the solution without vortex changes. Finally, this point belongs to $\kappa_3(d)$ since the energy of the bifurcated solution is zero for both eigenfunctions, in particular for the vortex solution. We want to point out that a similar analysis for the intersection of these curves has been performed in [1] in the one-dimensional setting and it yields to a solvability condition of fourth-order at the point of intersection.

The aspect ratio. As we have said, d is the characteristic size of the rectangle, but we have not taken into account the variations in the aspect ratio. In fact, the shape of the curves $\kappa_i(d)$ are independent of the aspect ratio. Only the values of the limits when d and κ are small depend on it.

Indeed, when the aspect ration gets very large, the problem is reduced to a one-dimensional problem studied in [3]. The curves $\kappa_i(d)$ found in [3] have exactly the same shape as here and the regions R_i are similar. Only the asymptotic limits in the case κ and d small will change and the value of the constant such that $\kappa d =$ constant for the definition of κ_2 and κ_4. Nevertheless, for large d, the limits of the curve κ_3 is the same, i.e. 0.4 and this is related to the same eigenvalue problem.

5. Conclusion

We have obtained very detailed bifurcation diagrams for the Ginzburg–Landau model of a two-dimensional cross-section of a three-dimensional superconducting cylinder when the applied field is along the direction of the axis. Detailed analysis are provided for the solution branches in the different regions of the (κ, d) plane. What distinguishes the different regions are features like the existence (or the lack of existence) of vortex solutions, the global and local stability of solutions, and the hysteresis phenomena. We note that the analysis includes regions with

small and hysteresis phenomena. We note that the analysis includes regions with small and intermediate values of κ which is not often featured in the existing studies, as most of the works in the literature focus on the vortex state which appears for larger values of κ or for thin films. Though we have computed the bifurcation diagrams with rectangular cross-sections, they are very representative of the general cases. Naturally, for small samples, the geometric conditions may have a stronger effect on leading to detailed alternations to the bifurcation curves. A change of topology, such as rings or shells, may present other complications [6] but we expect similar bifurcation diagrams remain valid. In addition, comparisons with existing theories have been made in the paper. Some remaining questions have also been raised.

Acknowledgements

This work was made possible thanks to the joint research project France Hong Kong (Procore) grant.

References

[1] A. Aftalion, S.J. Chapman, Asymptotic analysis of a secondary bifurcation of the one-dimensional Ginzburg–Landau equations of superconductivity, SIAM J. Appl. Math. 60 (4) (2000) 1157–1176.
[2] A. Aftalion, E.N. Dancer, On the symmetry and uniqueness of solutions of the Ginzburg–Landau equations for small domains, Com. Contemp. Math. 3 (1) (2001) 1–14.
[3] A. Aftalion, W.C. Troy, On the solutions of the one-dimensional Ginzburg–Landau equations for superconductivity, Physica D 132 (1999) 214–232.
[4] E. Akkermans, K. Mallick, Vortices in Ginzburg–Landau billiards, J. Phys. A 32 (41) (1999) 7133–7143.
[5] L. Almeida, F. Bethuel, in preparation.
[6] B. Baelus, F.M. Peeters, V.A. Schweigert, Vortex states in superconducting rings, Phy. Rev. B 61 (2000) 9734–9747.
[7] P. Bauman, D. Phillips, Q. Tang, Stable nucleation for the Ginzburg–Landau system with an applied magnetic field, Arch. Rational Mech. Anal. 142 (1) (1998) 1–43.
[8] A. Bernoff, P. Sternberg, Onset of superconductivity in decreasing fields for general domains, J. Math. Phys. 39 (1998) 1272–1284.
[9] C. Bolley, B. Helffer, An application of semi-classical analysis to the asymptotic study of the supercooling field of a superconducting material, Ann. Inst. Henri Poincaré (Phys. Théorique) 58 (1993) 189–233.
[10] S.J. Chapman, Q. Du, M.D. Gunzburger, A variable thickness thin film model for superconductivity, Z. Angew. Math. Phys. 47 (1996) 410–431.
[11] S.J. Chapman, Q. Du, M.D. Gunzburger, J.S. Peterson, Simplified Ginzburg–Landau models for superconductivity valid for high kappa and high fields, Adv. Math. Sci. Appl. 5 (1) (1995) 193–218.
[12] S.J. Chapman, S.D. Howison, J.R. Ockendon, Macroscopic models of superconductivity, SIAM Rev. 34 (4) (1992) 529–560.
[13] M. Del Pino, P. Felmer, P. Sternberg, Ginzburg–Landau, Boundary concentration for eigenvalue problems related to the onset of superconductivity, Com. Math. Phys. 210 (2000) 413–446.
[14] P. Deo, F.M. Peeters, V.A. Schweigert, Mesoscopic superconducting disks, Superlattices Microst. 25 (1999) 1195–1211.
[15] P. Deo, V.A. Schweigert, F.M. Peeters, A.K. Geim, Phys. Rev. Lett. 79 (1997) 4653–4656.
[16] Q. Du, Discrete gauge invariant approximations of a time-dependent Ginzburg–Landau model of superconductivity, Math. Comp. 67 (1998) 965–986.
[17] Q. Du, P. Gray, High-kappa limit of the time dependent Ginzburg–Landau model for superconductivity, SIAM J. Appl. Math. 56 (1996) 1060–1093.
[18] Q. Du, M.D. Gunzburger, J.S. Peterson, Analysis and approximation of the Ginzburg–Landau model of superconductivity, SIAM Rev. 34 (1) (1992) 54–81.
[19] Q. Du, M.D. Gunzburger, J.S. Peterson, Computational simulation of type-II superconductivity including pinning phenomena, Phys. Rev. B 51 (1995) 16194–16203.
[20] P.G. De Gennes, Superconductivity of Metals and Alloys, Addison-Wesley, Reading, MA, 1966.
[21] V.L. Ginzburg, On the destruction and onset of superconductivity in a magnetic field, Soviet Phys. JETP 34 (1958) 78–87.
[22] V.L. Ginzburg, L.D. Landau, On the theory of superconductivity, Soviet Phys. JETP 20 (1950) 1064–1082 [English Trans.: D. ter Haar (Ed.), Men of Physics: L.D. Landau, Pergamon Press, Oxford, 1965, 138–167].
[23] T. Giorgi, D. Phillips, The breakdown of superconductivity due to strong fields for the Ginzburg–Landau model, SIAM J. Math. Anal. 30 (1999) 341–359.
[24] B. Helffer, A. Morame, Magnetic bottles in connection with superconductivity, Preprint, 2000.
[25] B. Helffer, X. Pan, Upper critical field and location of surface nucleation of superconductivity, Preprint, 2001.
[26] Q. Li, Z. Wang, Q. Wang, Vortex structure for a d + s-wave superconductor, Phys. Rev. B 59 (1999) 613–618.
[27] F. Lin, Q. Du, Ginzburg–Landau vortices: dynamics, pinning and hysteresis, SIAM J. Math. Anal. 28 (1997) 1265–1293.
[28] K. Lu, X. Pan, Estimates of the upper critical field for the Ginzburg–Landau equations of superconductivity, Physica D 127 (1–2) (1999) 73–104.
[29] K. Lu, X. Pan, Eigenvalue problems of Ginzburg–Landau operator in bounded domains, J. Math. Phys. 40 (6) (1999) 2647–2670.

[30] K. Lu, X. Pan, Surface nucleation of superconductivity in 3 dimensions. Special issue in celebration of Jack K. Hale's 70th birthday, Part 2 (Atlanta, GA/Lisbon, 1998), J. Differ. Equations 168 (2) (2000) 386–452.
[31] X. Pan, Surface superconductivity in applied magnetic field above H_{c_2}, Preprint, 2001.
[32] D. Saint-James, P.G. De Gennes, Onset of superconductivity in decreasing fields, Phys. Lett. 7 (1963) 306–307.
[33] E. Sandier, S. Serfaty, Global minimizers for the Ginzburg–Landau functional below the first critical magnetic field, Ann. Inst. H. Poincare Anal. Non-lineaire 17 (1) (2000) 119–145.
[34] S. Serfaty, Local minimizers for the Ginzburg–Landau energy near critical magnetic field, Commun. Contemp. Math. 1 (1999) 213–254 and 295–333.
[35] S. Serfaty, Stable configurations in superconductivity: uniqueness, multiplicity, and vortex-nucleation, Arch. Ration. Mech. Anal. 149 (4) (1999) 329–365.
[36] V.A. Schweigert, F.M. Peeters, Phase transitions in thin mesoscopic superconducting disks, Phys. Rev. B 57 (1998) 13817–13832.
[37] V.A. Schweigert, F.M. Peeters, P.S. Deo, Vortex phase diagram for mesoscopic superconducting disks, Phys. Rev. Lett. 81 (1998) 2783–2786.
[38] M. Tinkham, Introduction to Superconductivity, McGraw-Hill, New York, 1975.
[39] Q. Wang, Z. Wang, Vortex state and dynamics of a d-wave superconductor: finite-element analysis, Phys. Rev. B 55 (1997) 11756–11765.